Genes to Cells

WILEY

Genes to Cells

ORIGINAL ARTICLE OPEN ACCESS

Cryo-EM Analysis of a Unique Subnucleosome Containing Centromere-Specific Histone Variant CENP-A

Osamu Kawasaki[1] | Yoshimasa Takizawa[2,3] | Iori Kiyokawa[1] | Hitoshi Kurumizaka[2,4,5] | Kayo Nozawa[1]

[1]School of Life Science and Technology, Institute of Science Tokyo, Yokohama, Kanagawa, Japan | [2]Laboratory of Chromatin Structure and Function, Institute for Quantitative Biosciences, The University of Tokyo, Tokyo, Japan | [3]Department of Computational Biology and Medical Sciences, Graduate School of Frontier Sciences, The University of Tokyo, Tokyo, Japan | [4]Department of Biological Sciences, Graduate School of Science, The University of Tokyo, Tokyo, Japan | [5]Laboratory for Transcription Structural Biology, RIKEN Center for Biosystems Dynamics Research, Yokohama, Japan

Correspondence: Hitoshi Kurumizaka (kurumizaka@iqb.u-tokyo.ac.jp) | Kayo Nozawa (nozawa.k.d544@m.isct.ac.jp)

Received: 29 January 2025 | **Revised:** 5 March 2025 | **Accepted:** 12 March 2025

Transmitting Editor: Hiroshi Kimura

Funding: This work was supported by the Japan Society for the Promotion of Science (JSPS) KAKENHI grants (JP20K06599, JP21H05154, JP22K06098, JP23H02519, JP23H05475, JP24H02319, and JP24H02328), the Japan Science and Technology Agency (JPMJCR24T3, JPMJER1901, and JPMJFR224Z), and the Japan Agency for Medical Research and Development (JP24ama121002 and JP24ama121009).

Keywords: CENP-A | centromere | cryo-EM structure | histone | nucleosome

ABSTRACT

In eukaryotes, genomic DNA is stored in the nucleus as nucleosomes, in which a DNA segment is wrapped around a protein octamer consisting of two each of the four histones, H2A, H2B, H3, and H4. The core histones can be replaced by histone variants or altered with covalent modifications, contributing to the regulation of chromosome structure and nuclear activities. The formation of an octameric histone core in nucleosomes is widely accepted. Recently, the H3–H4 octasome, a novel nucleosome-like structure with a histone octamer consisting solely of H3 and H4, has been reported. CENP-A is the centromere-specific histone H3 variant and determines the position of kinetochore assembly during mitosis. CENP-A is a distant H3 variant sharing approximately 50% amino acid sequence with H3. In this study, we found that CENP-A and H4 also formed an octamer without H2A and H2B in vitro. We determined the structure of the CENP-A–H4 octasome at 3.66 Å resolution. In the CENP-A–H4 octasome, an approximately 120-base pair DNA segment was wrapped around the CENP-A–H4 octameric core and displayed the four CENP-A RG-loops, which are the direct binding sites for another centromeric protein, CENP-N.

1 | Introduction

The basic unit of chromatin is the nucleosome core particle, composed of two copies of each of the four core histones, H2A, H2B, H3, and H4, together with an approximately 145 base-pair (bp) DNA fragment (Luger et al. 1997). The nucleosome is structurally versatile and contains different types of histone variants and histone modifications, as well as distinct histone stoichiometries (Kurumizaka et al. 2021; Luger et al. 2012). The resulting DNA compaction upon nucleosome formation limits the accessibility of the genomic DNA and affects essential cellular processes, such as transcription, replication, and repair (Lai and Pugh 2017). In our recent study, we determined the cryo-EM structure of an unconventional nucleoprotein particle called the H3–H4 octasome, consisting solely of H3 and H4, without H2A and H2B (Nozawa et al. 2022). We have additionally confirmed the presence of the H3–H4 octasome in budding yeast cells through in vivo protein crosslinking experiments. However, the genomic location and function of the H3–H4 octasome in cells have remained unclear.

Centromeres provide the assembly site for the kinetochore, to which microtubules are attached during chromosome segregation in the mitotic phase of the cell cycle and are dictated by the centromere-specific histone H3 variant, CENP-A. The key function of the CENP-A nucleosome appears to be the recruitment of other centromere-specific proteins, such as the constitutive centromere-associated network (CCAN) complex (Nagpal and Fierz 2021). The CCAN complex consists of 16 subunits and is dynamically assembled at the centromere during the G1, S, and early G2 phases. Among the subunits of the CCAN complex, CENP-N and CENP-C recognize CENP-A in chromatin and promote the assembly of the other CCAN subunits onto the CENP-A nucleosome. Depletion and overexpression of CENP-A have been demonstrated to induce mitotic abnormalities and high CENP-A expression levels are frequently found in various cancers (Saha et al. 2020).

The CENP-A nucleosome has been biochemically and structurally defined in vitro (Furuyama and Henikoff 2009; Dalal et al. 2007; Sekulic et al. 2010; Black et al. 2004; Tachiwana et al. 2011; Roulland et al. 2016; Falk et al. 2016; Takizawa et al. 2020; Yatskevich et al. 2022). A nucleosome-sized region of DNA within the centromere is reportedly protected from nuclease activity, suggesting the presence of a nucleosome-like structure in vivo (Furuyama and Biggins 2007). Additionally, recent high-resolution protein mapping of the budding yeast genome has revealed that while CENP-A/Cse4 is robustly detected in the core centromeric region, other histones are not clearly observed (Rossi et al. 2021). Furthermore, it has been suggested that the H2A and H2B in nucleosomes are scarce at the centromere region of budding yeast (Mizuguchi et al. 2007). These findings may support the presence of CENP-A–H4 octasomes in centromeric chromatin.

In this study, we reconstituted the CENP-A–H4 octasome in vitro and solved its cryo-EM structure with human CENP-A and H4. The CENP-A–H4 octasome structure comprises four CENP-A–H4 dimers assembled in an octameric core, wrapped by approximately 120 bp of DNA with flexible ends. This DNA length in the CENP-A–H4 octasome is consistent with the previous in vivo and the conventional CENP-A nucleosome containing H2A and H2B (Cole et al. 2011; Krassovsky et al. 2012). The CENP-A–H4 octasome presented in this study has two times (four) the number of RG-loops, which are the target sites for CENP-N, as compared to the CENP-A nucleosome. These characteristics of the CENP-A–H4 octasome may provide an advantage for the assembly of the CENP-A binding proteins and contribute to kinetochore assembly in centromeres.

2 | Results and Discussion

2.1 | Reconstitution of the CENP-A–H4 Octasome

We reconstituted the nucleosome-like particle with human histones CENP-A and H4 in the presence of a 145 bp DNA fragment containing the Widom 601 nucleosome positioning sequence by the salt dialysis method (Thåström et al. 1999). The reconstituted CENP-A–H4 octasome was detected by native polyacrylamide gel electrophoresis (PAGE), and its histone stoichiometry was analyzed by SDS PAGE (Figure 1A,B). To evaluate the histone-DNA interactions within the CENP-A–H4 octasome, we conducted a nuclease sensitivity assay, comparing the CENP-A–H4 octasome with the canonical nucleosome, H3–H4 octasome, and CENP-A nucleosome as controls (Figure 1C). Micrococcal nuclease (MNase), an endonuclease and exonuclease, preferentially digests DNA regions that are not tightly bound to histones while sparing DNA that remains securely wrapped around histones (Noll 1974). Time-course analysis of MNase digestion demonstrated that the canonical nucleosome protects a prominent 145 bp DNA fragment, representing nucleosomal DNA that is tightly wrapped, as well as a smaller ~120 bp fragment at later stages, which indicates partial unwrapping of DNA ends (Figure 1C, lanes 2–5; Koopmans et al. 2009). As reported previously, in the H3–H4 octasome, ~120 and ~80 bp DNA fragments were protected from MNase digestion (Figure 1C, lanes 6–9; Nozawa et al. 2022). This may be consistent with the DNA end flexibility and specific MNase susceptible sites in the H3–H4 octasome structure. In the CENP-A nucleosome, a ~100 bp DNA fragment was protected in addition to ~120 and ~80 bp fragments (Figure 1C, lanes 10–13). Interestingly, the MNase susceptibility profiles of the CENP-A–H4 octasome and the CENP-A nucleosome were quite similar (Figure 1C, lanes 14–17). This suggests that the accessibilities of the DNA wrapped in the CENP-A–H4 octasome and the CENP-A nucleosome are comparable. The ~80 bp DNA fragment protection by the H3–H4 octasome likely corresponds to the H3–H4 tetrasome unit (Zou et al. 2018). Therefore, the ~80 bp DNA fragments observed in the CENP-A–H4 octasome and the CENP-A nucleosome may represent a footprint of the CENP-A–H4 tetrasome unit.

2.2 | Structural Analysis of the CENP-A–H4 Octasome

We then performed the cryo-EM single particle analysis and determined the structure of the CENP-A–H4 octasome at 3.66 Å resolution (Figure 2A, Figure S1A–F, Table S1). The purified CENP-A–H4 octasome sample was analyzed with a 300 kV electron microscope. Approximately 8.7 million particles related to the CENP-A–H4 octasome were identified from 11,430 electron micrographs. A structural comparison of the CENP-A–H4 octasome with the CENP-A nucleosome revealed the features that are conserved and specific to CENP-A–H4 octasome. A ~120 bp DNA segment is wrapped around the octameric CENP-A–H4 core 1.5 times in a left-handed manner, resembling the CENP-A nucleosome. Our structure of the CENP-A–H4 octasome comprising the Widom 601 DNA sequence had flexible DNA ends, which were also observed in the reported structures of the CENP-A nucleosome containing an alpha-satellite (a repetitive human centromeric DNA) sequence (Tachiwana et al. 2011) or a Widom 601 sequence (Boopathi et al. 2020). Unlike the CENP-A nucleosome, the CENP-A–H4 octasome lacks the acidic patch provided by H2A and H2B, which serves as a docking site for nucleosome binding proteins, including histone modifiers and nucleosome remodelers (Sundaram and Vasudevan 2020) (Figure 2B). The CENP-A–H4 octasome adopts a clamshell-like conformation, consisting of two stacked disks connected by an H4–H4′

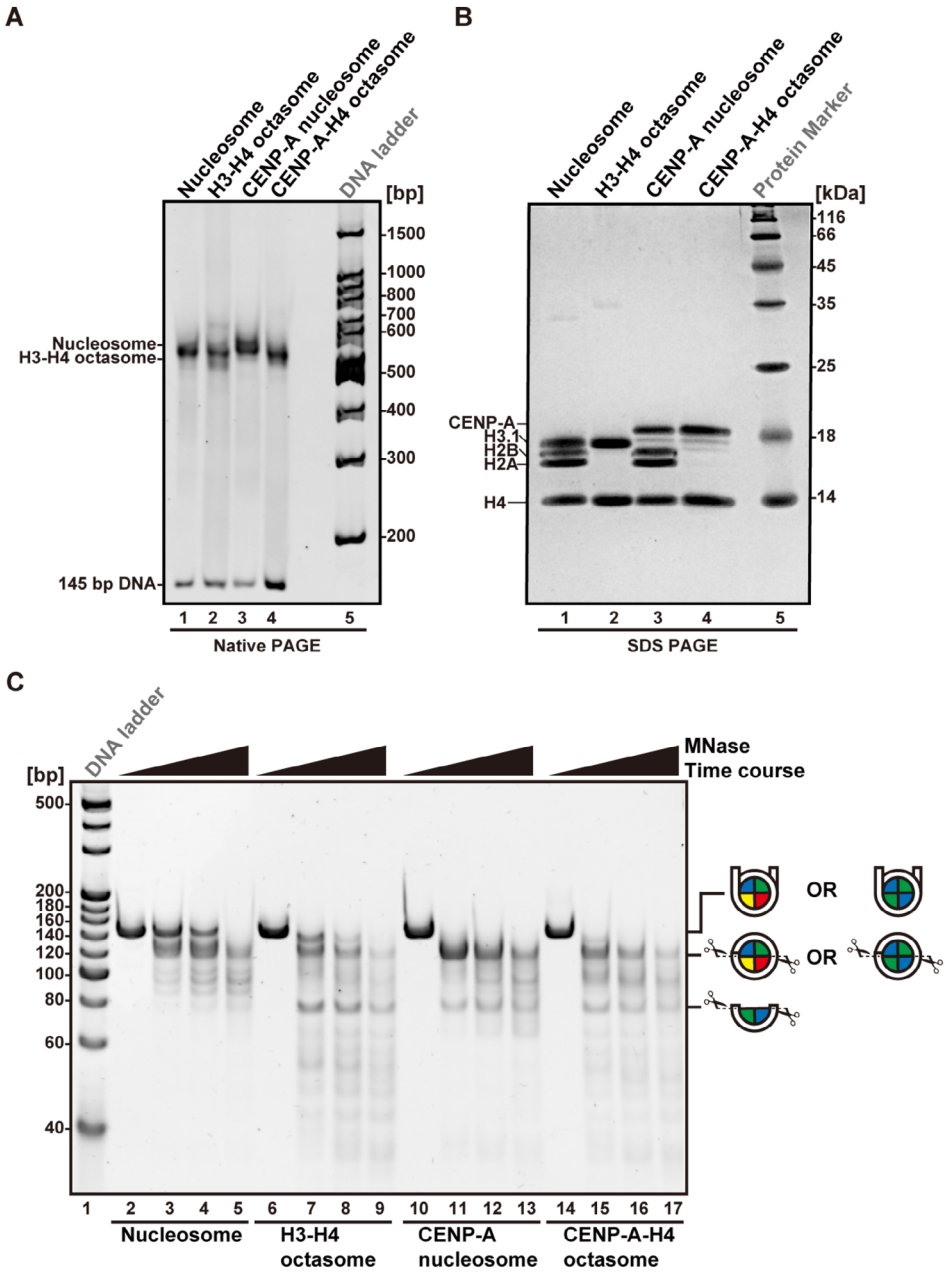

FIGURE 1 | Reconstitution of the CENP-A–H4 octasome. The reconstitution of the purified nucleosome, H3–H4 octasome, CENP-A nucleosome, and CENP-A–H4 octasome was performed using human histones and a 145-bp Widom 601 positioning sequence. These complexes were analyzed by (A) native PAGE with ethidium bromide (EtBr) staining to assess DNA integrity and (B) SDS-PAGE with Coomassie Brilliant Blue (CBB) staining to confirm the presence of histones. (C) The indicated nucleoprotein samples were subjected to MNase digestion for 0, 15, 30, and 60 min (from left to right). Following MNase treatment, the DNA was separated from histones and analyzed by native PAGE with EtBr staining. The MNase sensitivity assay was repeated three times to ensure the reproducibility of the results.

four-helix bundle. This structural arrangement closely resembles that of the H3–H4 octasome; however, it differs from the CENP-A nucleosome (Figure 2A,C). The distance between the two DNA gyres in the CENP-A–H4 octasome was ~20 Å wider than that of the CENP-A nucleosome. This is probably due to the lack of the H2A-mediated L1–L1′ interaction and the presence of the unobserved CENP-A αN regions in the inter-disk space. This difference in the DNA conformations between the CENP-A nucleosome and the CENP-A–H4 octasome may affect the higher-order conformations of chromatin fibers in centromeres.

The CENP-A–H4 octasome contains four CENP-A copies that are recognized by CENP-A binding proteins, such as CENP-N and CENP-C (Carroll et al. 2009; Kato et al. 2013). Therefore, the CENP-A–H4 octasome provides twice the number of binding sites for CENP-A binding proteins. Especially, CENP-A contains the RG-loop with two residues (Arg80 and Gly 81) inserted in the L1 loop connecting α1 and α2 (Tachiwana et al. 2011). The CENP-A–H4 octasome structure revealed that the four copies of RG-loops are completely exposed to the solvent (Figure 2D). Since the CENP-N N-terminal domain directly binds to the RG-loop (Pentakota et al. 2017; Chittori et al. 2018; Allu et al. 2019),

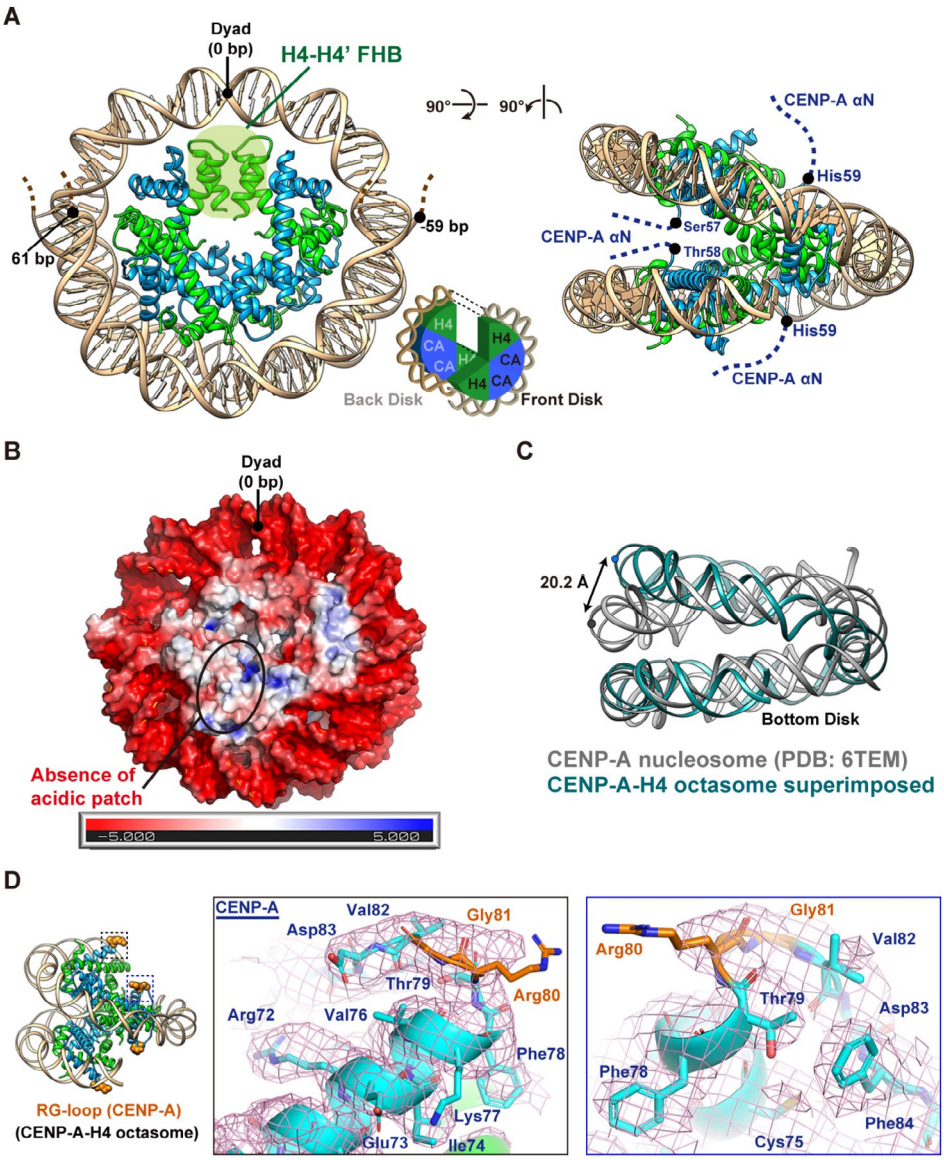

FIGURE 2 | Cryo-EM structure of the CENP-A–H4 octasome. (A) The cryo-EM structure of the CENP-A–H4 octasome. The electron densities of the N-terminal regions of CENP-A and the DNA termini were not observed (indicated by dashed lines). CA: CENP-A; FHB: four-helix bundle. (B) Surface electrostatic potentials map of the CENP-A–H4 octasome. (C) The ribbon model of the CENP-A–H4 octasome and that of the CENP-A nucleosome are aligned by the bottom disk. The dots mark Position 39 in both DNA strands, while the double arrow highlights the variation in measured distances between the DNA gyres in these structures. (D) Close-up cryo-EM map of two CENP-A RG-loops on one side of the CENP-A–H4 octasome. The EM map was post-processed using the DeepEMhancer software (Sanchez-Garcia et al. 2021). Similar electron densities of the RG-loops were clearly observed on the opposite side.

the CENP-A–H4 octasome could be targeted by CENP-N more efficiently than the CENP-A nucleosome. Further studies will be needed to test this possibility.

2.3 | A Model for CENP-N Binding to the CENP-A–H4 Octasome

The CENP-A nucleosome is known to bind to CENP-C and CENP-N, and their complex structures have been reported (Ali-Ahmad et al. 2019; Allu et al. 2019; Pentakota et al. 2017; Chittori et al. 2018). While CENP-C requires binding to both the acidic patch of the H2A–H2B dimer and the C-terminal tail of CENP-A to recognize the CENP-A nucleosome, CENP-N primarily recognizes CENP-A by binding to the CENP-A RG loop and the adjacent DNA (Allu et al. 2019). Recently, a new DNA binding site was found on CENP-N, and CENP-N reportedly promoted the stacking of CENP-A nucleosomes and formed a characteristic centromeric chromatin structure, even in the absence of other CCAN components (Zhou et al. 2022). We performed a model fitting of CENP-N on the CENP-A–H4 octasome, using this CENP-A–N nucleosome complex composed of Widom 601 DNA and the C-terminal 50 amino acid deletion mutant, CENP-N$^{1–289}$ (PDB: 7U4D).

As a result, the CENP-N on the RG-loop is found at superhelical location (SHL) (+2.5) of the CENP-A nucleosome, whereas it is predicted to be positioned at SHL (−0.5) and/or SHL (+5.5)

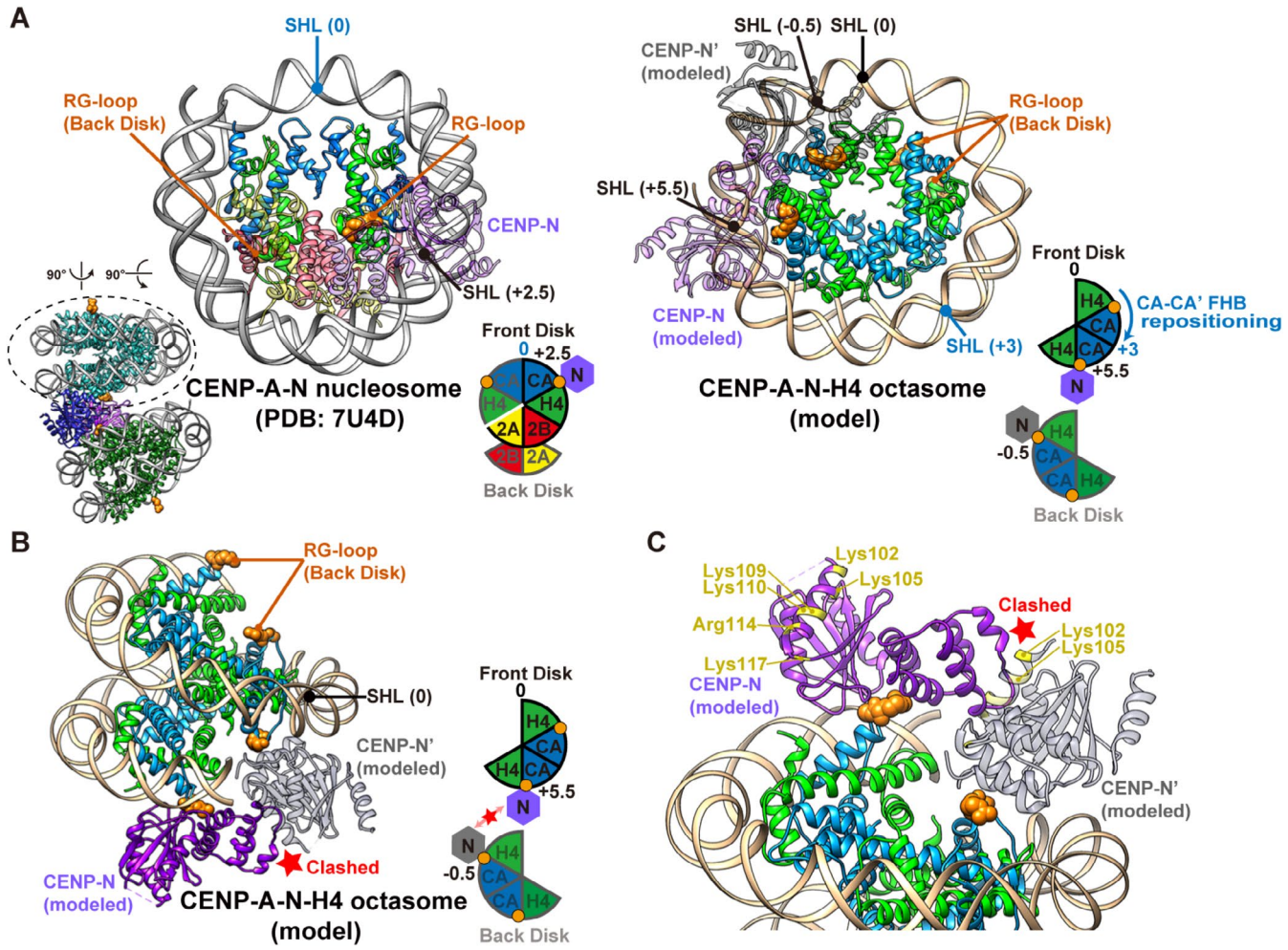

FIGURE 3 | Structural comparison of the CENP-A-N nucleosome and CENP-A-N-H4 octasome models. (A) Ribbon models of the CENP-A-N nucleosome (left panel) and the CENP-A-N-H4 octasome modeled by superimposition of the CENP-A-N structure from PDB ID: 7U4D (right panel). Locations of the CENP-A Arg80 and Gly81 residues in those structures are shown as orange spheres. The CENP-A–H4 octasome has twice as many RG-loops as compared to the CENP-A nucleosome. The RG-loops in the CENP-A-N-H4 octasome are positioned three helical turns away from the RG-loops in the CENP-A nucleosome, that is, superhelical locations (SHLs) +5.5 and −0.5 compared to +2.5. The white line between H4 and H2A in the CENP-A nucleosome schematic emphasizes that the two proteins are not connected. (B) Ribbon model of the CENP-A-N-H4 octasome, viewed from the side. Each of the two exposed RG-loops on one side of the CENP-A–H4 octasome potentially binds to CENP-N, but the superimposition suggests a clash between the two molecules. (C) Close-up of two CENP-Ns in the CENP-A-N-H4 octasome complex model, viewed from the back side. The positively charged residues in the α6 helix of CENP-N that are utilized in nucleosomal DNA stacking in CENP-A-N nucleosome complexes are shown in yellow.

in the CENP-A–H4 octasome, due to the repositioning of the CENP-A-CENP-A′ four-helix bundle (Figure 3A). There are two exposed RG-loops on each face of the CENP-A–H4 octasome. Two CENP-N molecules superimposed on the two sites on the same face apparently clash, suggesting that a CENP-N molecule can potentially bind to either site (Figure 3B). However, previous studies have demonstrated that CENP-N adopts various distinct conformations to bind to different binding partners during the assembly of the CCAN complex (Yatskevich et al. 2022), suggesting that structural transformations may allow two CENP-N molecules to bind on the same face of the CENP-A–H4 octasome.

The CENP-N-mediated stacking of CENP-A nucleosomes occurs through a series of positively charged amino acids (Lys102, Lys105, Lys109, Lys110, Arg114, and Lys117) located on the same face of the α6 helix. These residues of CENP-N, mapped on the superimposed structure, are exposed to the solvent for possible higher-order structure formation (Figure 3C). Therefore, the CENP-A–H4 octasome may play a role in the formation of the characteristic higher-order chromatin structure at the centromere.

3 | Conclusion

We successfully reconstituted the CENP-A–H4 octasome and solved its cryo-EM structure at 3.66 Å resolution. Like the CENP-A nucleosome, the CENP-A–H4 octasome contained an approximately 120-bp DNA segment and the exposed RG-loops of CENP-A, a common foothold for centromeric proteins. The CENP-N binding RG-loops were exposed at different sites from those on the CENP-A nucleosome, suggesting the distinct epigenetic function of the CENP-A–H4 octasome. Defining how CENP-N and other CCAN proteins bind to the CENP-A–H4 octasome in vivo and how they differ from the interactions with

the CENP-A nucleosome will be important to clarify kinetochore formation during mitosis.

4 | Experimental Procedures

4.1 | Purification of DNA Fragments

A 145 bp DNA fragment corresponding to the Widom 601 sequence (5′-ATCAGAATCCCGGTGCCGAGGCCGCTCAATTGGTCGTAGACAGCTCTAGCACCGCTTAAACGCACGTACGCGCTGTCCCCCGCGTTTTAACCGCCAAGGGGATTACTCCCTAGTCTCCAGGCACGTGTCAGATATATACATCGAT-3′) was prepared as previously described (Dyer et al. 2003). Tandem repeats of this fragment were cloned into the pGEM-T Easy vector (Promega), which was subsequently amplified in *Escherichia coli* and purified. The DNA fragment was excised by digestion with EcoRV (Takara), and the vector DNA was removed via polyethylene glycol (PEG) 6,000 precipitation.

4.2 | Preparation of Human Histones, Histone Complexes, and Nucleosomes

Human histones H2A, H2B, H3.1, CENP-A, and H4 were expressed and purified following an established protocol (Arimura et al. 2012). Histone octamers, H3–H4 tetramers, and CENP-A–H4 tetramers were refolded through dialysis and purified using gel filtration chromatography with a HiLoad 16/600 Superdex 200 pg. column (Cytiva). The H3–H4 and CENP-A–H4 octasomes were reconstituted by combining tetramers with a 145 bp Widom 601 DNA fragment and refolding through the salt dialysis method, as described in previous studies (Arimura et al. 2012). For reconstitution, the DNA and histones were mixed at a molar ratio of 1:2.2 in 2 M KCl buffer. The nucleoprotein complexes were dialyzed against a buffer containing 10 mM Tris–HCl (pH 7.5), 2 M KCl, 1 mM EDTA, and 1 mM dithiothreitol (DTT), with the KCl concentration gradually reduced to 0.25 M using a peristaltic pump. The assembled octasomes were incubated at 55°C for 2 h and subsequently purified using 6% polyacrylamide native PAGE with a Prep Cell apparatus (Bio-Rad).

4.3 | MNase Treatment Assay

Nucleosomes containing 145 bp DNA (200 ng each) were incubated with 0.01 unit/μL MNase (Takara) at 37°C for 0, 15, 30, and 60 min in a reaction buffer composed of 50 mM Tris–HCl (pH 7.5), 2.5 mM $CaCl_2$, 1.9 mM DTT, and 50 mM NaCl. The MNase reactions were stopped by adding a quenching buffer containing 20 mM Tris–HCl (pH 7.5), 20 mM EDTA, 0.5 mg/mL proteinase K, and 0.25% SDS. The resulting DNA fragments were purified through phenol/chloroform extraction and ethanol precipitation, followed by analysis on a 10% polyacrylamide native PAGE in 0.5× TBE buffer (45 mM Tris base, 45 mM boric acid, and 1 mM EDTA).

4.4 | Cryo-EM Sample Preparation and Data Collection

To stabilize the purified CENP-A–H4 octasome, the gradient fixation method (GraFix) was employed during sucrose gradient centrifugation, following an approach (Kastner et al. 2008). A linear sucrose gradient was prepared using a Gradient Master instrument (SKB). The low-density buffer contained 20 mM HEPES-KOH (pH 7.5), 1 mM DTT, and 10% (w/v) sucrose, while the high-density buffer included 20 mM HEPES-KOH (pH 7.5), 1 mM DTT, 25% (w/v) sucrose, and 3% paraformaldehyde. Centrifugation was carried out at 27,000 rpm for 16 h at 4°C using an SW41 rotor (Beckman Coulter). Fractions containing the CENP-A–H4 octasome were subjected to buffer exchange using Micro Bio-Spin Columns (Bio-Rad) equilibrated with 20 mM Tris–HCl (pH 7.5) and 1 mM DTT.

For cryo-EM sample preparation, 2 μL of the CENP-A–H4 octasome solution (0.57 mg/mL) was applied to a glow-discharged Quantifoil R1.2/1.3200-mesh Cu grid. After blotting for 6 s under 100% humidity at 12°C using a Vitrobot Mark IV system (Thermo Fisher Scientific, USA), the grids were rapidly frozen in liquid ethane. Cryo-EM data collection was conducted using SerialEM software (Mastronarde 2005) on a Krios G4 cryo-electron microscope (Thermo Fisher Scientific, USA) operated at 300 kV, with a pixel size of 1.06 Å and a defocus range of −1.25 to −2.5 μm. Imaging was performed at an electron flux of 11.5 e^-/pix/s with a 6-s exposure time using an energy-filtered K3 direct electron detector (Gatan, USA) in electron counting mode, with a 25 eV slit width. Each dataset comprised 40 frames, with a total dose of approximately 57.3 $e^-/Å^2$.

4.5 | Cryo-EM Image Processing

A total of 11,430 micrographs of the CENP-A–H4 octasome were aligned using the MotionCor2 software (Zheng et al. 2017), with dose weighting applied. The contrast transfer function (CTF) parameters for each micrograph were determined using CTFFIND4 (Rohou and Grigorieff 2015). Image processing of the CENP-A–H4 sample was carried out using RELION 3.1 following the procedure (Zivanov et al. 2018). Initially, 8,697,848 particles were automatically picked using the 2D template-based picker and subjected to reference-free 2D classification to remove poor-quality particles. From this, 3,097,901 selected particles were used for 3D classification, applying a global soft mask. The best 3D classes were selected based on resolution. The structures were subjected to 3D refinement, Bayesian polishing, and two rounds of CTF refinement. The final resolution of the refined CENP-A–H4 octasome map was 3.66 Å, as determined by the gold standard Fourier Shell Correlation (FSC) method with the 0.143 criteria (Scheres 2016). The final map was visualized using UCSF Chimera software (Pettersen et al. 2004). Data collection and processing statistics for the CENP-A–H4 octasome structure are summarized in Table S1.

4.6 | Model Building

The structural model of the CENP-A–H4 octasome was built from the cryo-EM structure of the CENP-A–H4 octasome containing *Homo sapiens* histones H3 and H4 and a 145 bp Widom 601 DNA fragment (PDB: 7X57) (Nozawa et al. 2022). The amino acid residues of H3 were adjusted to those of human CENP-A. The model coordinates were refined automatically with phenix.real_space_refine (Adams et al. 2010) and manually using Coot (Emsley et al. 2010). All structure figures were prepared

using UCSF Chimera and PyMOL (Schrödinger; http://www.pymol.org).

Author Contributions

Osamu Kawasaki: investigation, validation, formal analysis, writing – original draft, writing – review and editing, data curation. **Yoshimasa Takizawa:** investigation, validation, formal analysis, data curation, writing – original draft, writing – review and editing, funding acquisition. **Iori Kiyokawa:** data curation, investigation, validation, formal analysis, writing – original draft, writing – review and editing. **Hitoshi Kurumizaka:** investigation, data curation, funding acquisition, writing – original draft, writing – review and editing, methodology, supervision, project administration, resources, conceptualization. **Kayo Nozawa:** conceptualization, methodology, data curation, supervision, formal analysis, validation, investigation, funding acquisition, project administration, resources, writing – review and editing, writing – original draft.

Acknowledgments

We are grateful to the members of the Kurumizaka Laboratory and Nozawa Laboratory, particularly Chizuru Sogawa, Yukari Iikura, Yas Takeda, and Atsuko Watanabe, for their assistance. We thank Masahide Kikkawa (The University of Tokyo) for cryo-EM data collection.

Conflicts of Interest

The authors declare no conflicts of interest.

Data Availability Statement

The cryo-EM reconstructions and atomic models of the CENP-A–H4 octasome have been deposited in the Electron Microscopy Data Bank and the Protein Data Bank (PDB) under the following accession codes: EMD-62193 and 9K9L, respectively.

References

Adams, P. D., P. V. Afonine, G. Bunkóczi, et al. 2010. "PHENIX: A Comprehensive Python-Based System for Macromolecular Structure Solution." *Acta Crystallographica Section D: Biological Crystallography* 66: 213–221.

Ali-Ahmad, A., S. Bilokapić, I. B. Schäfer, M. Halić, and N. Sekulić. 2019. "CENP-C Unwraps the Human CENP-A Nucleosome Through the H2A C-Terminal Tail." *EMBO Reports* 20: e48913.

Allu, P. K., J. M. Dawicki-McKenna, T. Van Eeuwen, et al. 2019. "Structure of the Human Core Centromeric Nucleosome Complex." *Current Biology* 29: 2625–2639.e5.

Arimura, Y., H. Tachiwana, T. Oda, M. Sato, and H. Kurumizaka. 2012. "Structural Analysis of the Hexasome, Lacking One Histone H2A/H2B Dimer From the Conventional Nucleosome." *Biochemistry* 51: 3302–3309.

Black, B. E., D. R. Foltz, S. Chakravarthy, K. Luger, V. L. Woods, and D. W. Cleveland. 2004. "Structural Determinants for Generating Centromeric Chromatin." *Nature* 430: 578–582.

Boopathi, R., R. Danev, M. Khoshouei, et al. 2020. "Phase-Plate Cryo-EM Structure of the Widom 601 CENP-A Nucleosome Core Particle Reveals Differential Flexibility of the DNA Ends." *Nucleic Acids Research* 48: 5735–5748.

Carroll, C. W., M. C. C. Silva, K. M. Godek, L. E. T. Jansen, and A. F. Straight. 2009. "Centromere Assembly Requires the Direct Recognition of CENP-A Nucleosomes by CENP-N." *Nature Cell Biology* 11: 896–902.

Chittori, S., J. Hong, H. Saunders, et al. 2018. "Structural Mechanisms of Centromeric Nucleosome Recognition by the Kinetochore Protein CENP-N." *Science* 359: 339–343.

Cole, H. A., B. H. Howard, and D. J. Clark. 2011. "The Centromeric Nucleosome of Budding Yeast Is Perfectly Positioned and Covers the Entire Centromere." *Proceedings of the National Academy of Sciences of the United States of America* 108, no. 12: 12,687–12,692.

Dalal, Y., H. Wang, S. Lindsay, and S. Henikoff. 2007. "Tetrameric Structure of Centromeric Nucleosomes in Interphase *Drosophila* Cells." *PLoS Biology* 5: e218.

Dyer, P. N., R. S. Edayathumangalam, C. L. White, et al. 2003. "Reconstitution of Nucleosome Core Particles From Recombinant Histones and DNA." *Methods in Enzymology* 375: 23–44.

Emsley, P., B. Lohkamp, W. G. Scott, and K. Cowtan. 2010. "Features and Development of Coot." *Acta Crystallographica Section D: Biological Crystallography* 66: 486–501.

Falk, S. J., J. Lee, N. Sekulic, M. A. Sennett, T.-H. Lee, and B. E. Black. 2016. "CENP-C Directs a Structural Transition of CENP-A Nucleosomes Mainly Through Sliding of DNA Gyres." *Nature Structural & Molecular Biology* 23: 204–208.

Furuyama, S., and S. Biggins. 2007. "Centromere Identity Is Specified by a Single Centromeric Nucleosome in Budding Yeast." *Proceedings of the National Academy of Sciences of the United States of America* 104, no. 14: 14,706–14,711.

Furuyama, T., and S. Henikoff. 2009. "Centromeric Nucleosomes Induce Positive DNA Supercoils." *Cell* 138: 104–113.

Kastner, B., N. Fischer, M. M. Golas, et al. 2008. "GraFix: Sample Preparation for Single-Particle Electron Cryomicroscopy." *Nature Methods* 5: 53–55.

Kato, H., J. Jiang, B.-R. Zhou, et al. 2013. "A Conserved Mechanism for Centromeric Nucleosome Recognition by Centromere Protein CENP-C." *Science* 340: 1110–1113.

Koopmans, W. J. A., R. Buning, T. Schmidt, and J. van Noort. 2009. "spFRET Using Alternating Excitation and FCS Reveals Progressive DNA Unwrapping in Nucleosomes." *Biophysical Journal* 97: 195–204.

Krassovsky, K., J. G. Henikoff, and S. Henikoff. 2012. "Tripartite Organization of Centromeric Chromatin in Budding Yeast." *Proceedings of the National Academy of Sciences of the United States of America* 109: 243–248.

Kurumizaka, H., T. Kujirai, and Y. Takizawa. 2021. "Contributions of Histone Variants in Nucleosome Structure and Function." *Journal of Molecular Biology* 433: 166–678.

Lai, W. K. M., and B. F. Pugh. 2017. "Understanding Nucleosome Dynamics and Their Links to Gene Expression and DNA Replication." *Nature Reviews. Molecular Cell Biology* 18: 548–562.

Luger, K., M. L. Dechassa, and D. J. Tremethick. 2012. "New Insights Into Nucleosome and Chromatin Structure: An Ordered State or a Disordered Affair?" *Nature Reviews. Molecular Cell Biology* 13: 436–447.

Luger, K., A. W. Mäder, R. K. Richmond, D. F. Sargent, and T. J. Richmond. 1997. "Crystal Structure of the Nucleosome Core Particle at 2.8 Å Resolution." *Nature* 389: 251–260.

Mastronarde, D. N. 2005. "Automated Electron Microscope Tomography Using Robust Prediction of Specimen Movements." *Journal of Structural Biology* 152: 36–51.

Mizuguchi, G., H. Xiao, J. Wisniewski, M. M. Smith, and C. Wu. 2007. "Nonhistone Scm3 and Histones CenH3-H4 Assemble the Core of Centromere-Specific Nucleosomes." *Cell* 129: 1153–1164.

Nagpal, H., and B. Fierz. 2021. "The Elusive Structure of Centro-Chromatin: Molecular Order or Dynamic Heterogenetity?" *Journal of Molecular Biology* 433: 166–676.

Noll, M. 1974. "Subunit Structure of Chromatin." *Nature* 251: 249–251.

Nozawa, K., Y. Takizawa, L. Pierrakeas, et al. 2022. "Cryo–Electron Microscopy Structure of the H3-H4 Octasome: A Nucleosome-Like

Particle Without Histones H2A and H2B." *Proceedings of the National Academy of Sciences of the United States of America* 119: e2206542119.

Pentakota, S., K. Zhou, C. Smith, et al. 2017. "Decoding the Centromeric Nucleosome Through CENP-N." *eLife* 6: e33442.

Pettersen, E. F., T. D. Goddard, C. C. Huang, et al. 2004. "UCSF Chimera? A Visualization System for Exploratory Research and Analysis." *Journal of Computational Chemistry* 25: 1605–1612.

Rohou, A., and N. Grigorieff. 2015. "CTFFIND4: Fast and Accurate Defocus Estimation From Electron Micrographs." *Journal of Structural Biology* 192: 216–221.

Rossi, M. J., P. K. Kuntala, W. K. M. Lai, et al. 2021. "A High-Resolution Protein Architecture of the Budding Yeast Genome." *Nature* 592: 309–314.

Roulland, Y., K. Ouararhni, M. Naidenov, et al. 2016. "The Flexible Ends of CENP-A Nucleosome Are Required for Mitotic Fidelity." *Molecular Cell* 63: 674–685.

Saha, A. K., R. Contreras-Galindo, Y. S. Niknafs, et al. 2020. "The Role of the Histone H3 Variant CENPA in Prostate Cancer." *Journal of Biological Chemistry* 295: 8537–8549.

Sanchez-Garcia, R., J. Gomez-Blanco, A. Cuervo, J. M. Carazo, C. O. S. Sorzano, and J. Vargas. 2021. "DeepEMhancer: A Deep Learning Solution for Cryo-EM Volume Post-Processing." *Communications Biology* 4: 874.

Scheres, S. H. W. 2016. "Processing of Structurally Heterogeneous Cryo-EM Data in RELION." *Methods in Enzymology* 579: 125–157.

Sekulic, N., E. A. Bassett, D. J. Rogers, and B. E. Black. 2010. "The Structure of (CENP-A–H4)2 Reveals Physical Features That Mark Centromeres." *Nature* 467: 347–351.

Sundaram, R., and D. Vasudevan. 2020. "Structural Basis of Nucleosome Recognition and Modulation." *BioEssays* 42, no. 1: e1900234.

Tachiwana, H., W. Kagawa, T. Shiga, et al. 2011. "Crystal Structure of the Human Centromeric Nucleosome Containing CENP-A." *Nature* 476: 232–235.

Takizawa, Y., C.-H. Ho, H. Tachiwana, et al. 2020. "Cryo-EM Structures of Centromeric Tri-Nucleosomes Containing a Central CENP-A Nucleosome." *Structure* 28: 44–53.e4.

Thåström, A., P. T. Lowary, H. R. Widlund, H. Cao, M. Kubista, and J. Widom. 1999. "Sequence Motifs and Free Energies of Selected Natural and Non-Natural Nucleosome Positioning DNA Sequences." *Journal of Molecular Biology* 288: 213–229.

Yatskevich, S., K. W. Muir, D. Bellini, et al. 2022. "Structure of the Human Inner Kinetochore Bound to a Centromeric CENP-A Nucleosome." *Science* 376: 844–852.

Zheng, S. Q., E. Palovcak, J.-P. Armache, K. A. Verba, Y. Cheng, and D. A. Agard. 2017. "MotionCor2: Anisotropic Correction of Beam-Induced Motion for Improved Cryo-Electron Microscopy." *Nature Methods* 14: 331–332.

Zhou, K., M. Gebala, D. Woods, et al. 2022. "CENP-N Promotes the Compaction of Centromeric Chromatin." *Nature Structural & Molecular Biology* 29: 403–413.

Zivanov, J., T. Nakane, B. O. Forsberg, et al. 2018. "New Tools for Automated High-Resolution Cryo-EM Structure Determination in RELION-3." *eLife* 7: e42166.

Zou, T., F. Hashiya, Y. Wei, Z. Yu, G. N. Pandian, and H. Sugiyama. 2018. "Direct Observation of H3-H4 Octasome by High-Speed AFM." *Chemistry: A European Journal* 24, no. 15: 15,998–16,002.

Supporting Information

Additional supporting information can be found online in the Supporting Information section.